Effect of varying water content and applied voltage on the performance of electroosmotic dewatering

Nilan Jayasiri[1*], *Andy* Fourie[1], and *Cristina* Vulpe[2]

[1] Department of Civil, Environmental and Mining Engineering, The University of Western Australia, Perth, WA, 6009, Australia.
[2] Department of Mechanical Engineering, The University of Western Australia, Perth, WA, 6009, Australia.

Abstract. Electroosmotic (EO) dewatering is a technology that may be employed for the treatment of fine-grained soils with undesirable geotechnical characteristics, such as high compressibility and low undrained shear strengths. Historically, the soil types that have been subjected to EO treatment encompass a broad variety of soils ranging from soft clays with initial water contents close to the liquid limit to low solids content slurries (e.g., dredged sludge and slurry deposited tailings), which typically have a water content far higher than the liquid limit. Despite being a fundamental factor that governs the consolidation behaviour of each soil type, the effect of variation of the pre-treatment water content, to the overall performance of the EO treatment process, has not been quantified. In this study, EO dewatering laboratory-scale experiments were performed considering three consistency levels, corresponding to the water content values of 1, 1.5 and 2 times the liquid limit. The results indicated that the effectiveness of the EO treatment increased with the increase in pre-treatment water content, in terms of proportion of water removed and relative strength gain changes. A major finding of the present study is that the EO dewatering effectiveness significantly increases after the water content of the material increases beyond 1.5 times the liquid limit. Additionally, a new approach to evaluate the energy consumption is presented. The influence of adopted voltage gradient and initial water content on the energy consumption is then evaluated using the results of this study.

1 Introduction

Rapid urbanisation has compelled engineers to carry out infrastructure development projects over soil deposits that have undesirable geotechnical characteristics, such as high compressibility and low undrained shear strengths [1]. These soil deposits typically include natural soft soils such as soft marine clays, peat and alluvial clay deposits, and hydraulically placed soils such as slurried tailings and dredged materials. Natural soft soils often differ from hydraulically placed material in terms of engineering behaviour. When characterised by the as-measured water content relative to the liquid limit, natural soft clays typically have a water content close to the liquid limit, whereas the hydraulically placed low solids content slurries typically have a water content far higher than the liquid limit. Owing to resulting low bearing capacities and excessive settlement characteristics, these problematic soils often undergo some form of ground improvement to render them suitable for development.

Electrically-assisted dewatering, using the concept of electroosmosis [2], has demonstrated promising results for the treatment of fine-grained soils [3–6]. This ground improvement strategy involves the application of an electrical field using a series of electrodes to induce the movement of water molecules from the positively charged electrodes towards the negatively charged electrodes. If the accumulated water at the cathode electrodes is subsequently drained away, this process facilitates consolidation of the material bounded by the electrodes. This process is known as electroosmotic dewatering. The electroosmotic (EO) flow through soils can be represented by:

$$q_e = k_e \frac{\Delta V}{L} A \tag{1}$$

where, q_e is the flow rate, k_e is the EO permeability, V is the applied voltage difference between electrodes, L is the distance between electrodes and A is the cross-sectional area perpendicular to the flow.

Review of literature suggests that, to date, EO treatment has been adopted for the treatment of a variety of fine-grained soils with varying water contents. Bjerrum [4] performed EO dewatering to strengthen Norwegian quick clay prior to performing an excavation. Bergardo et al. [7] carried out EO consolidation experiments on Bangkok soft clay, while Kaniraj and Yee [8] used an organic soil in their experiments. A number of studies investigated the potential use of EO dewatering for the treatment of slurried tailings with extremely high water contents [3,9–11]. Despite being a fundamental factor that governs the consolidation behaviour of each soil type, the effect of variation of the pre-treatment water content on the overall performance of the EO treatment process

* Corresponding author: nilan.jayasiri@research.uwa.edu.au

is not well quantified. To this end, the present study focused on investigating the effect of varying water content and applied voltage on the performance of EO dewatering in greater detail, based on the investigation by Jayasiri et al. [12]. This study further expands upon the investigations conducted by Jayasiri et al. [12,13] to evaluate the influence of adopted voltage gradient and initial water content on energy consumption. Additionally, several different scanning electron microscopy (SEM) imaging techniques were used to investigate the changes in the microfabric induced by the EO treatment. The strengths and limitations of each approach are also discussed.

2 Materials and methods

2.1 Materials

Powder kaolin processed by SUVO minerals – Pittong operations in Australia was used in the experiments. Characterisation of kaolin, including main index and XRD tests have been previously performed by Jayasiri et al. [12,14]. In summary, kaolin clay has a specific gravity of 2.6, a liquid limit of 74% and a plastic limit of 44%. The material is predominantly composed of clay-sized particles, accounting for approximately 70% of the total composition.

2.2 Test setup

A plastic tub with approximately 20 L capacity was used to perform the EO dewatering experiments. Electrokinetic geosynthetics (EKGs) were used for both anode and cathode electrodes, which were positioned approximately 380 mm apart (L), adjacent to the walls of the tub (Fig. 1). Previous studies have shown that the use of EKGs results in improving the EO dewatering process, which could otherwise be affected by the corrosion of conventional metal electrodes [3,15]. Drainage of the accumulated water in the vicinity of the cathode was facilitated by using a perforated tube located next to the cathode. The drained water was collected in a measuring cylinder, and the water volume was recorded at periodic intervals. The electrical field was applied using a constant voltage configuration [16], with a direct current benchtop power supply. The current was monitored throughout the test duration.

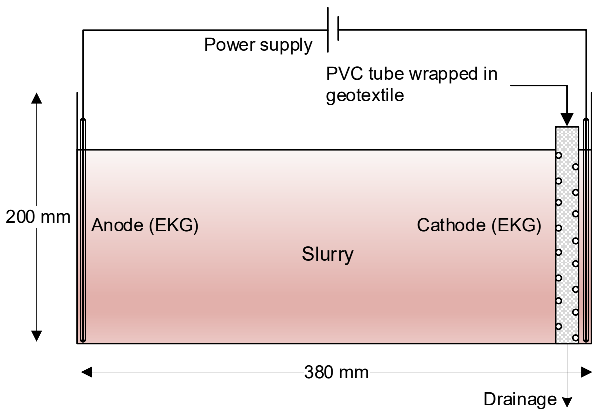

Fig. 1. Schematic of the laboratory experimental setup.

2.3 Test procedure

EO dewatering experiments were performed considering three consistency levels, corresponding to water content values of 1, 1.5 and 2 times the liquid limit. Additionally, three voltage values were adopted corresponding to 50, 100 and 150 V/m voltage gradient values. The summary of the experimental program is outlined in Table 1, while the test procedure is briefly described below:

1. Slurry specimens required for the experiments were prepared by mixing powder kaolin with deionized water. Required volume of water was determined based on the weight-volume relationships, corresponding to the water content values of 1, 1.5 and 2 times the liquid limit (Table 1).
2. The tub was filled with the kaolin mix in layers while preventing the formation of macro voids. Prior to filling, the electrodes were placed inside the tub to minimise disturbance. After filling, the initial wet mass of each slurry specimen was approximately 22 kg.
3. Experiments were commenced by connecting the pertinent electrodes to the power supply. A plastic film was used to cover the tub to prevent moisture loss through evaporation.
4. Tests were continued until the flowrate became essentially zero.
5. Upon termination of the tests, undrained shear strength values were measured using a hand vane apparatus.
6. Samples were recovered to determine the water content and for SEM imaging.

Table 1. Summary of experiments (modified after Jayasiri et al. [12]).

Test ID	Water content ratio[a]	Water content (%)	Voltage gradient (V/m)	Voltage (V)
LL1-EK50	1	78	50	19
LL1-EK100	1	79	100	38
LL1-EK150	1	78	150	57
LL1.5-EK50	1.5	114	50	19
LL1.5-EK100	1.5	115	100	38
LL1.5-EK150	1.5	115	150	57
LL2-EK50	2	150	50	19
LL2-EK100	2	151	100	38
LL2-EK150	2	150	150	57

[a]*Water content relative to the liquid limit.*

3 Results

3.1 Drainage volume

Fig. 2 (a) illustrates the temporal change in proportion of drained water volume ($V_{d,LLx-EKy}/V_{i,LLx-EKy}$), which is defined as the ratio of water removed ($V_{d,LLx-EKy}$) relative to the initial amount of water present ($V_{i,LLx-EKy}$) in each of the nine tests, with $x = [1,1.5,2]$

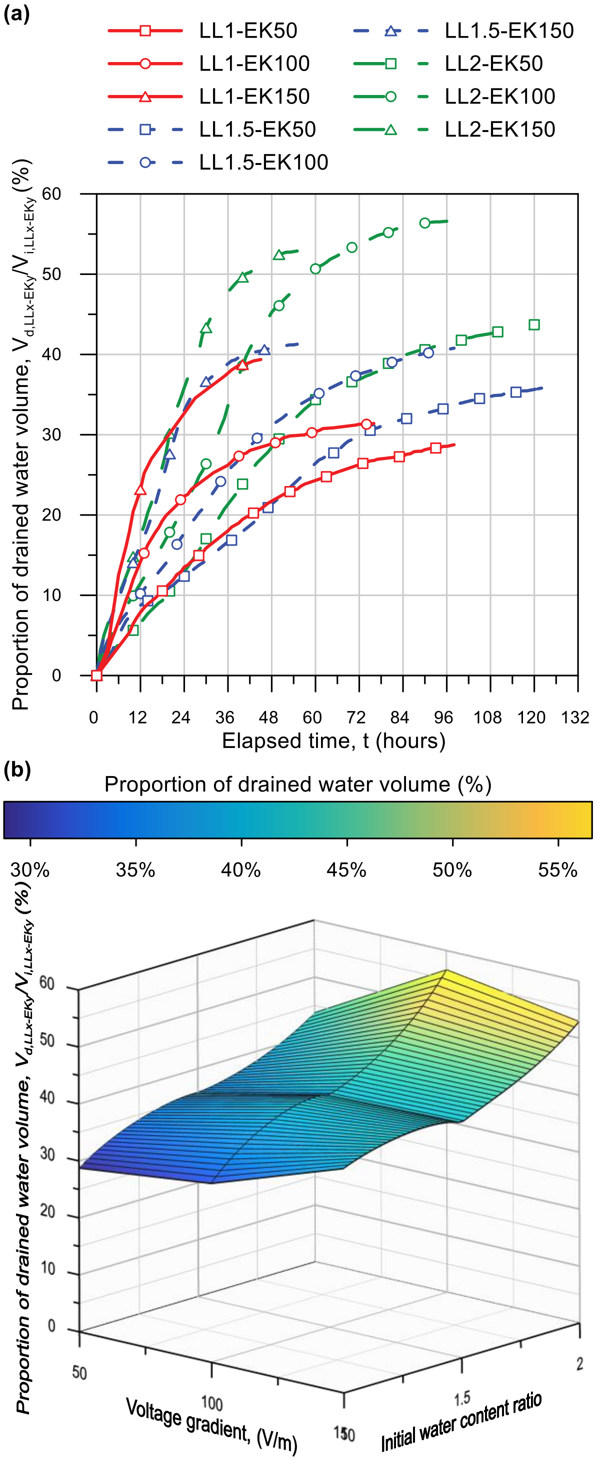

Fig. 2. (a) Proportion of drained water volume; (b) Surface plot showing the effect of varying water content and applied voltage on the drained water volume (modified after Jayasiri et al. [12]).

initial water content ratio and $y = [50,100,150]$ V/m voltage gradient. Overall, at the end of EO treatment, the proportion of drained water volume for the experiments conducted in this study ranged between approximately 25% to 55%. The experiments conducted with an initial water content of two times the liquid limit exhibited the highest proportion of drained water volume, while the lowest proportion of water volume was observed in the experiments commenced at the water content equal to the liquid limit. The Helmholtz - Smoluchowski model describes that EO flow occurs due to the movement of hydrated cations [17,18]. Given that water is a polar molecule (partial negative and a partial positive charge), they typically combine with cations in the electrical double layer to form hydrated cations. Therefore, the movement of cations due to the application of an electrical current also causes the surrounding water molecules to move towards the cathode. Given that more water molecules were available in the LL2 experiments to form hydrated cations, the observed recovery of a higher proportion of drained water volume could be essentially due to the higher initial water content. As interpreted in Fig. 2 (b), the effectiveness of the EO treatment, in terms of the proportion of water removed, increased with the increase in pre-treatment water content, regardless of the applied voltage. Interestingly, the EO dewatering effectiveness significantly increases after the water content of the material increases beyond 1.5 times the liquid limit. The observed behaviour suggests that EO treatment may be particularly effective for the treatment of soil deposits with extremely high water contents such as hydraulically placed materials.

In accordance with Eq. (1), the increasing voltage gradient generally resulted in a higher proportion of drained water volume, although the intermediate voltage gradient (100 V/m) led to the highest proportion of drained water volume in the LL2 experiment series. No significant difference was observed in the end of treatment drained water volumes in LL2 and LL1.5 experiments conducted using 100 and 150 V/m potential gradients. Therefore, intermediate voltage gradients are adequate for treating high water content soils, while high voltage gradients could be adopted to enhance dewatering volumes of low water content soil deposits, if required.

3.2 Water content

At the end of the treatment process, water content values were determined at five different locations located between the electrodes (x) for each of the experiments. The absolute change in water content ($\Delta w_{LLx-EKy}$), normalised by the initial water content ($w_{i,LLx-EKy}$), for each experiment is shown in Fig. 3 as a percentage, where:

$$\Delta w_{LLx-EKy} = w_{f,LLx-EKy} - w_{i,LLx-EKy} \qquad (2)$$

with $w_{f,LLx-EKy}$ is the final water content and $w_{i,LLx-EKy}$ is the initial water content for each of the

 https://doi.org/10.1051/e3sconf/202673004012

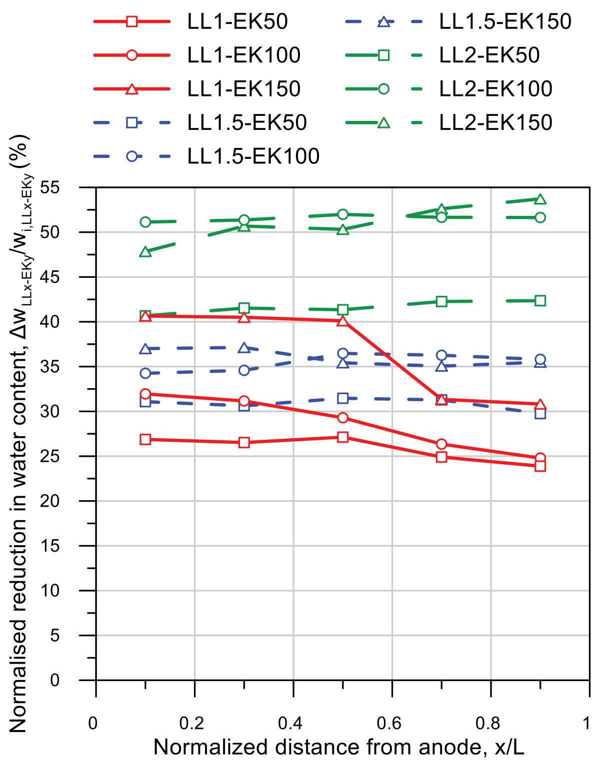

Fig. 3. Normalised reduction in water content between the electrodes (modified after Jayasiri et al. [12]).

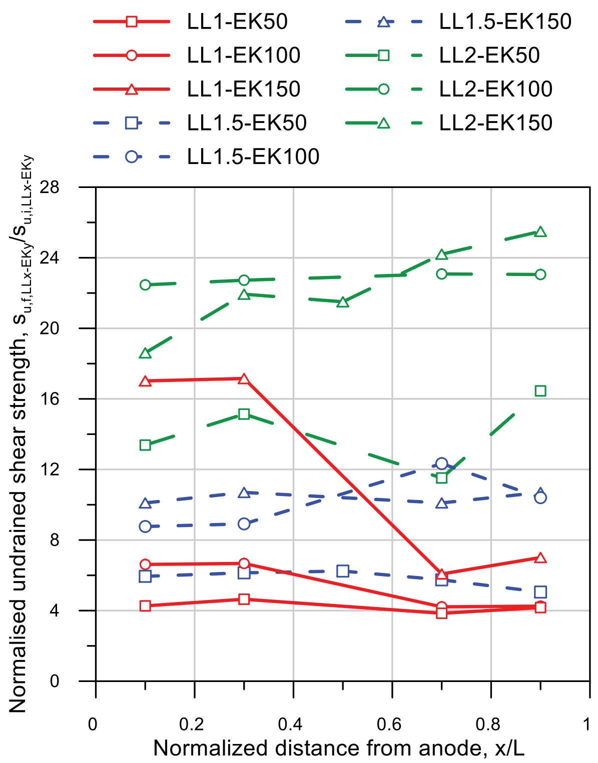

Fig. 4. Normalised undrained shear strength between the electrodes (modified after Jayasiri et al. [12]).

nine EO tub tests. Here, x and y denote the initial water content ratio and voltage gradient values adopted in each of the nine tests.

The overall relative change in normalised water content for the experiments conducted in this study varied from 25% to 55%, in line with the proportion of drained water volumes noted earlier. On average, LL1 and LL2 experiments demonstrated a 30% and 34% relative decrease in water content, respectively, while LL2 experiments exhibited a relatively higher reduction in water content (48%). The observed behaviour among the experiments conducted at three different consistency levels further suggests that the EO dewatering effectiveness significantly increases after the initial water content of the material exceeds 1.5 times the liquid limit.

The EO dewatering process usually creates an inhomogeneous water content profile, with the measured water content typically higher at the cathode compared to the anode. According to Fig. 3, a substantial difference among the post-treatment water content measurements cannot be observed in the present study, although some minor variation is evident in the LL1 experiment series. As noted by Jayasiri et al. [12], formation of shrinkage cracks in the soil mass between the anode and cathode is one of the primary reasons for the uneven water content profile caused by EO treatment.

3.3 Undrained shear strength

Undrained shear strength values were measured at five different locations located between the electrodes using a pocket shear vane apparatus. The ratio between the final and initial undrained shear strength values for each of the nine EO tub tests is presented in Fig. 4, where $s_{u,f,LLx-EKy}$ is the final undrained shear strength and $s_{u,i,LLx-EKy}$ is the initial undrained shear strength, with x and y denoting the initial water content ratio and voltage gradient values adopted in each of the nine tests. The $s_{u,i,LLx-EKy}$ values for LL1, LL1.5 and LL2 were approximately 2.4, 0.7 and 0.3 kPa, respectively. The observed trend in relative change in undrained shear strength generally agrees well with the relative water content changes discussed earlier. This behaviour was expected as the undrained shear strength is strongly influenced by the water content of remoulded clays.

Undrained shear strength is highly sensitive to the water content at low water contents (e.g., below the liquid limit) for remoulded clays [19]. Therefore, the absolute increase in undrained shear strength is greatest for the experiments conducted with the lowest initial water content (LL1). However, in terms of the relative increase, LL1 and LL1.5 experiments demonstrated seven- and nine-times in undrained shear strength, on average, respectively (Fig. 4). In contrast, EO treatment led to a twentyfold relative increase in undrained shear strength for LL2 experiment series. It is clear that the greatest relative improvement, in terms of strength gain was observed in the experiments performed with the poorest initial condition (LL2). This behaviour could be particularly beneficial when it comes to the ground improvement of soil deposits with extremely low strength characteristics such as slurried tailings and dredged sediments. Owing to the poor undrained shear characteristics of hydraulically deposited materials, it becomes challenging to implement conventional ground improvement approaches. For instance, wick drains coupled with surcharging may not be a feasible approach since placement of an earthen surcharge fill could be challenging due to the poor load bearing capacities of weak soil deposits. Therefore, a ground improvement approach that does not affect the total stress state of the material during the treatment process, such as an EO dewatering approach presents a very promising option to effectively treat soil deposits with high water contents.

3.4 Electric current

The electrical current measured during each experiment is depicted in Fig. 5. Regardless of the initial water content, an increasing voltage gradient led to a higher initial current in absolute values, almost suggesting a linear relationship. Although significant variability in current measurements was evident at early stages, the variability decreased as dewatering progressed, eventually approaching zero current measurement at culmination. In accordance with Ohm's law, the observed trend could be attributed to the material desaturation and subsequent increase in electrical resistance.

3.5 Energy consumption

Energy consumption during each experiment was calculated using the electric current measurements. For this purpose, the method proposed by Jayasiri et al. [13] was followed. One of the key benefits of this approach is its ability to take the degree of relative improvement induced by the EO treatment into account when determining the energy consumption. The extent of dewatering achieved is incorporated by considering the relative change in liquidity index ($\Delta I_L/I_{L,i}$) for each experiment, where $I_{L,i}$ is the is the initial liquidity index and ΔI_L is the absolute change in liquidity index. In contrast, for instance, other parameters such as water volume removed does not provide significant insights into the material response (with respect to the initial state) induced by the EO treatment. The use of liquidity

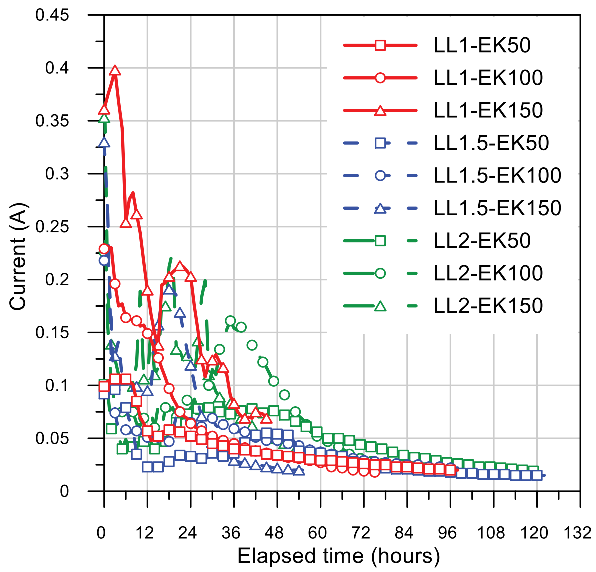

Fig. 5. Electric current measurements (after Jayasiri et al. [12]).

index also allows practitioners to evaluate the workability of the material, and furthermore, it can be used to correlate other important geotechnical parameters (e.g., undrained shear strength) using widely adopted empirical correlations. The general form of the normalised energy consumption, as proposed by Jayasiri et al. [13] is expressed as:

$$E_c^* = \frac{V \int_0^t I(t)\, dt}{W_s\ (I_{L,i} - I_{L,f})/I_{L,i}} \tag{3}$$

where, V is the voltage, I is the current, W_s is the soil mass based on dry basis, t is time, $I_{L,i}$ is the initial liquidity index and $I_{L,i}$ is the final liquidity index for each experiment.

The energy consumption calculations are outlined in Table 2 and the final rates for each of the nine experiments are graphically presented in Fig. 6. The initial liquidity index values of LL1, LL1.5 and LL2 were approximately 1.17, 2.39 and 3.62, respectively. Increasing the voltage gradient generally resulted in higher normalised changes in liquidity index, regardless of the initial water content. However, as presented in Fig. 6, the increasing voltage gradient also led to a higher normalised energy consumption, making the EO dewatering process less energy efficient. As noted earlier, increasing the voltage gradient from 100 V/m to 150 V/m did not increase the proportion of drained water volume for LL1.5 and LL2 experiments, and hence the normalised change in liquidity index (Table 2). However, to induce the same normalised change in liquidity index, higher voltage gradients consumed more energy. For instance, LL2-EK100 and LL2-EK150 experiments resulted in almost identical liquidity indices, but the energy consumed for the LL2-EK150 is approximately 11 kWhr/dry tonne higher than that of the LL2-EK100 experiment. From an economic perspective, the use of intermediate voltage gradients is recommended when treating high water content soils to reduce the operational costs, while high voltage gradients could be adopted to improve dewatering for low water content soil deposits, if required. Fig. 6 also suggests that, at a given voltage gradient, increasing initial water content generally resulted in consuming higher energy to induce a unit change in liquidity index of a unit of dry material.

3.6 Microstructure

Microstructure of the kaolin specimens before and after the EO treatment was studied using SEM imaging. Since conventional SEMs operate under a high vacuum, it is a fundamental step to dehydrate the specimens prior to imaging to prevent damage to the specimens and the equipment, which could be caused by moisture evaporation. Conventional practices such as oven drying or air drying the SEM specimens during preparation could result in artefacts in the microstructure due to suction induced disturbances, particularly if the specimens consist of clay-sized particles. To alleviate

Table 2: Energy consumption calculations.

Test ID	Initial WC	Initial liquidity index ($I_{L,i}$)	Final WC	Final liquidity index ($I_{L,f}$)	Normalised change in liquidity index ($\Delta I_L/I_{L,i}$)	Energy consumption (kWh/dry tonne)	Normalised energy consumption (kWhr/dry tonne)
LL1-EK50	78.3	1.16	58.8	0.49	0.58	6.16	10.71
LL1-EK100	79.3	1.19	56.1	0.40	0.66	15.43	23.24
LL1-EK150	78.4	1.16	49.8	0.18	0.84	36.54	43.44
LL1.5-EK50	114.4	2.39	79.6	1.20	0.50	7.15	14.38
LL1.5-EK100	114.7	2.40	73.5	0.99	0.59	16.58	28.26
LL1.5-EK150	114.3	2.39	72.7	0.97	0.59	24.03	40.39
LL2-EK50	150.3	3.61	87.7	1.48	0.59	12.37	20.94
LL2-EK100	150.7	3.63	73.2	0.98	0.73	28.28	38.78
LL2-EK150	150.1	3.61	73.6	1.00	0.72	35.98	49.74

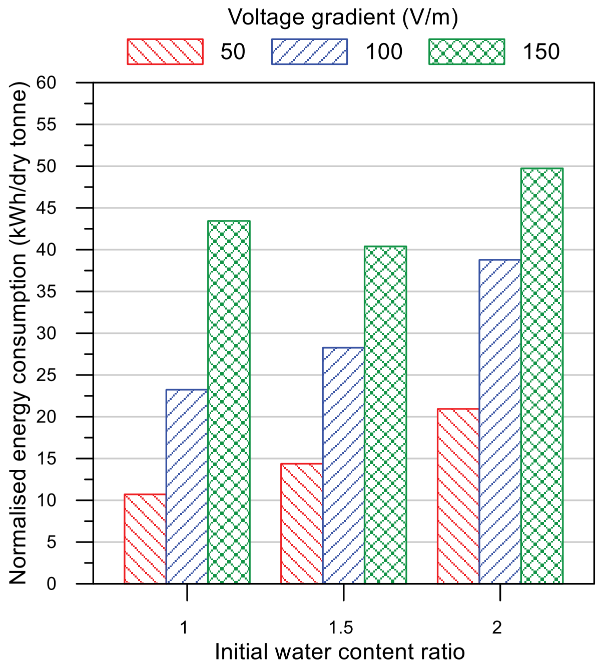

Fig. 6. Normalised energy consumption rates.

this issue, several cryogenic techniques were explored, as briefly outlined below:

1. Liquid nitrogen plunging: specimens were rapidly submerged in liquid nitrogen (-196°C) and freeze-dried (24 hours at -50°C) using sublimation, prior to SEM imaging under room temperature.
2. High pressure freezing (HPF): at first, specimen cryofixation was performed using a high-pressure freezer (pressure = 2100 bar, freezing rate = 24500°C/s). Subsequently, the specimens were freeze-dried for 24 hours at -50°C, before carrying out SEM imaging under room temperature.
3. CryoSEM: specimen cryofixation using high pressure freezing techniques was conducted following the same steps noted earlier. While submerged in liquid nitrogen, specimens were transferred to a cryo-preparation module to perform surface sublimation (10 minutes at -90 °C) and remove any frost contamination. Using a cryo-transfer unit, specimens were then transferred to a CryoSEM microscope to carry out imaging [12].

Of the three approaches considered, CryoSEM allows the investigation of frozen specimens that are in a hydrated state. Given that no drying is involved, this technique offers viewing the microstructure as close as possible to the native conditions with minimal artefacts. Although multiple steps are involved, specimen preparation and viewing can be done in a relatively short period compared to the other two methods. However, this technique requires specialised CryoSEM facilities, which are complex to operate and high in cost. Additionally, specimen handling can be technically demanding, requiring specialised training. The plunge-freezing technique is simple and less costly to perform. However, there is a greater likelihood of ice crystal formation and pore volume expansion during this process, which leads to artefacts, particularly when the water content of the specimen is high [20]. The HPF technique offers a superior preservation of microfabric in comparison to the plunging technique. High pressure and rapid freezing minimise pore volume expansion and ice crystal formation, which leads to minimal artefacts. One of the key benefits of the lyophilisation techniques (i.e., plunging and HPF) is that they allow imaging of the specimens using conventional SEMs that operate at room temperature. However, the specimens prepared by lyophilisation techniques can be extremely fragile, and therefore care must be taken when handling.

SEM images obtained for LL1-EK150 experiment using each approach are shown in Fig. 7. Images obtained using the HPF technique were comparable with those obtained from CryoSEM. In contrast, a visually apparent difference, in terms of the pore size, between the images produced using the plunging technique and CryoSEM can be seen, particularly in the untreated wet condition. As noted earlier, one of the main reasons for this behaviour could be due to pore volume expansion during freezing. The observations suggest that the HPF technique offers a reliable alternative to the CryoSEM, considering the complexity of carrying out CryoSEM imaging.

Regardless of the adopted approach, EO treatment resulted in alteration of the soil microfabric. The initial openly arranged particle structure changed to a face-to-face arrangement due to the EO treatment. The significant shrinkage in the void spaces and improved fabric could contribute to the enhanced engineering characteristics.

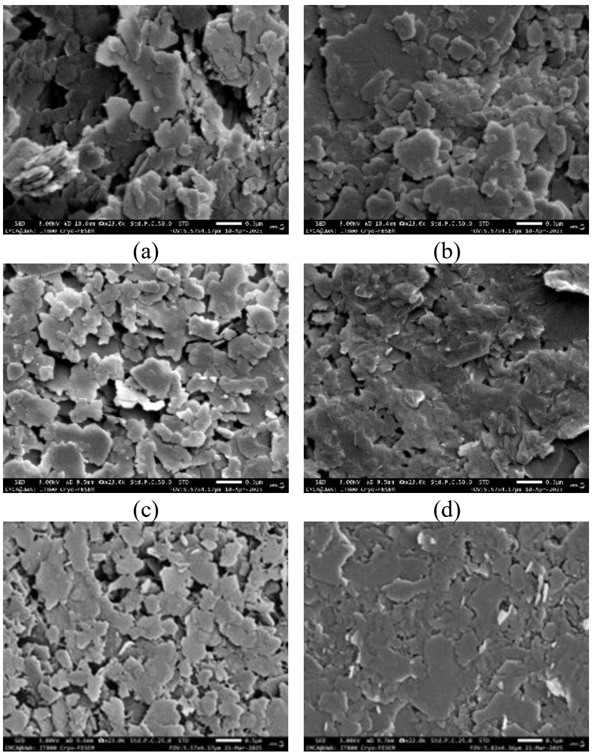

Fig. 7. SEM images (23.0k magnification) of LL1-EK150, obtained using (a) liquid nitrogen plunging (untreated); (b) liquid nitrogen plunging (EO treated); (c) HPF (untreated); (d) HPF (EO treated); (e) CryoSEM (untreated); (f) CryoSEM (EO treated).

4 Conclusions

This study focused on investigating the effect of varying water content and applied voltage on the performance of electroosmotic (EO) dewatering. In total, nine EO dewatering experiments were performed considering three consistency levels, corresponding to water content values of 1, 1.5 and 2 times the liquid limit. The results indicated that the effectiveness of the EO treatment increased with an increase in pre-treatment water content, in terms of the proportion of water removed, relative reduction in water content and relative undrained shear strength gain. The results also showed that the EO dewatering effectiveness significantly increases after the water content of the material increases beyond 1.5 times the liquid limit, making the EO treatment highly suitable for soils with high water contents. However, this came at the cost of low energy efficiency as energy consumption calculations showed that, compared to a low water content soil, high water content soils consumed more energy to induce a unit change in liquidity index of a unit of dry material, at a given voltage gradient.

The selection of commercially available kaolin as the testing material was based on its suitability for controlled sample preparation. Since kaolin is a clay with low activity, future work should consider extending this study to other clay types with higher activity.

The support received from Associate Professor Peta Clode in SEM imaging is gratefully acknowledged. This research was financially supported by the Australian Government through the Australian Research Council Linkage Project (LP200200216). The first author would like to acknowledge the Scholarship for International Research Fees, Ad Hoc Postgraduate Scholarship and MRIWA Postgraduate Top-up Scholarship supported by the University of Western Australia and Minerals Research Institute of Western Australia, respectively. In addition, the first author would like to acknowledge the financial support from Convocation of UWA Graduates provided through the Convocation Postgraduate Research Travel award.

References

1. B. Indraratna, A.S. Balasubramaniam, S. Balachandran, Performance of Test Embankment Constructed to Failure on Soft Marine Clay. J. Geotech. Eng. **118**, 12–33 (1992). https://doi.org/10.1061/(ASCE)0733-9410(1992)118:1(12)
2. F.F. Reuss, Charge-induced flow. Proceedings of the Imperial Society of Naturalists of Moscow, 1809 **3**, 327–344 (1809).
3. A.B. Fourie, D.G. Johns, C.F. Jones, Dewatering of mine tailings using electrokinetic geosynthetics. Can. Geotech. J. **44**, 160–172 (2007). https://doi.org/10.1139/t06-112
4. L. Bjerrum, J. Moum, O. Eide, Application of Electro-Osmosis to a Foundation Problem in a Norwegian Quick Clay. Géotechnique **17**, 214–235 (1967). https://doi.org/10.1680/geot.1967.17.3.214
5. S.R. Kaniraj, H.L. Huong, J.H.S. Yee, Electro-Osmotic Consolidation Studies on Peat and Clayey Silt Using Electric Vertical Drain. Geotech. Geol. Eng. **29**, 277–295 (2011). https://doi.org/10.1007/s10706-010-9375-8

6. H. Fu, Z. Fang, J. Wang, J. Chai, Y. Cai, X. Geng, J. Jin, F. Jin, Experimental comparison of electroosmotic consolidation of wenzhou dredged clay sediment using intermittent current and polarity reversal. Mar. Georesour. Geotechnol. **36**, 131–138 (2018). https://doi.org/10.1080/1064119X.2017.1326992
7. D. Bergado, I. Sasanakul, S. Horpibulsuk, Electro-Osmotic Consolidation of Soft Bangkok Clay Using Copper and Carbon Electrodes with PVD. Geotech. Test. J. **26**, 277–288 (2003). https://doi.org/10.1520/GTJ11309J
8. S.R. Kaniraj, J.H.S. Yee, Electro-Osmotic Consolidation Experiments on an Organic Soil. Geotech. Geol. Eng. **29**, 505–518 (2011). https://doi.org/10.1007/s10706-011-9399-8
9. J.Q. Shang, A.R. Fernando, E.K. Lam, Electrokinetic dewatering of gypsum containing tailings, in Tailings and Mine Waste 09: Proceedings of the Thirteenth International Conference on Tailings and Mine Waste, pp. 1–4 (2009).
10. S. Bourgès-Gastaud, P. Dolez, E. Blond, N. Touze-Foltz, Dewatering of oil sands tailings with an electrokinetic geocomposite. Miner. Eng. **100**, 177–186 (2017). https://doi.org/10.1016/j.mineng.2016.11.002
11. C. Du, B. Niu, F. Yi, M. Wang, X. Jiang, Electroosmosis of gold tailings under multiple electrokinetic geosynthetics electrodes. Geotext. Geomembr. **52**, 585–597 (2024). https://doi.org/10.1016/j.geotexmem.2024.03.002
12. N. Jayasiri, A. Fourie, C. Vulpe, Influence of initial water content and voltage gradient on electroosmotic dewatering of ultra-fine soils using novel electrokinetic geosynthetics. Geotext. Geomembr. **53**, 1623–1643 (2025). https://doi.org/10.1016/j.geotexmem.2025.08.006
13. N. Jayasiri, A. Fourie, C. Vulpe, A critical reappraisal of quantifying energy consumption during electroosmotic dewatering, Proc. Inst. Civ. Eng.: Ground. Improv. (under review).
14. N. Jayasiri, A. Fourie, C. Vulpe, Effects of Electroosmotic Treatment on Strength and Compressibility Behavior of an Ultra-fine Slurry, in Proceedings of Tailings and Mine Waste 2025, Banff, Alberta, Canada, (2025).
15. N. Jayasiri, A. Fourie, C. Vulpe, Utilization of novel electrokinetic geosynthetics for stabilization of ultra-fine tailings, in Proceedings of Tailings and Mine Waste 2024, Denver, Colorado, (2024).
16. N. Jayasiri, A. Fourie, C. Vulpe, A comparative study on the performance of electroosmotic consolidation of fluid fine tailings under constant voltage and constant current configurations, in Mine Closure 2024: Proceedings of the 17th International Conference on Mine Closure, Australian Centre for Geomechanics, Perth, (2024).
17. H.L.F. Von Helmholtz, Studies of electric boundary layers, Wied. Ann. **7**, 337–382 (1879).
18. M. Smoluchowski, In Graetz, L (Ed.) Handbuch der Elektrizitat und Magnetisums, (1914).
19. L. Bjerrum, Comparison of shear strength characteristics of normally consolidated clays, Norwegian Geotechnical Institute. Publication **35**, 13–22 (1960).
20. J. Du, R.A. Pushkarova, R.St.C. Smart, A cryo-SEM study of aggregate and floc structure changes during clay settling and raking processes. Int. J. Miner. Process. **93**, 66–72 (2009). https://doi.org/10.1016/j.minpro.2009.06.004